Available online at www.sciencedirect.com
ScienceDirect
Progress in Natural Science 19 (2009) 827–835
Progress in Natural Science
www.elsevier.com/locate/pnsc

Detection of dynamic brain networks modulated by acupuncture using a graph theory model

Lijun Bai [a], Wei Qin [a], Jie Tian [a,b,*], Jianping Dai [c], Wanhai Yang [a]

[a] *Life Science Research Center, School of Electronic Engineering, Xidian University, Xi'an 710071, China*
[b] *Medical Image Processing Group, Institute of Automation, Chinese Academy of Sciences, Beijing 100080, China*
[c] *Department of Radiology, Beijing Tiantan Hospital, Capital University of Medical Sciences, Beijing 100050, China*

Received 25 July 2008; received in revised form 4 September 2008; accepted 17 September 2008

Abstract

Neuroimaging studies involving acute acupuncture manipulation have already demonstrated significant modulatory effects on wide limbic/paralimbic nuclei, subcortical gray structures and the neocortical system of the brain. Due to the sustained effect of acupuncture, however, knowledge on the organization of such large-scale cortical networks behind the active needle stimulation phase is lacking. In this study, we originally adopted a network model analysis from graph theory to evaluate the functional connectivity among multiple brain regions during the post-stimulus phase. Evidence from our findings clearly supported the existence of a large organized functional connectivity network related to acupuncture function in the resting brain. More importantly, acupuncture can change such a network into a functional state underlying both pain perception and modulation, which is exhibited by significant changes in the functional connectivity of some brain regions. This analysis may help us to better understand the long-lasting effects of acupuncture on brain function, as well as the potential benefits of clinical treatments.

Keywords: Acupuncture; Brain network; Graph theory model; Functional magnetic resonance imaging (fMRI)

1. Introduction

Acupuncture, an ancient therapeutic technique, is currently gaining popularity as an important modality of alternative and complementary medicine in the West. In this process, the boundaries between East Asian medicines and biomedicine/science are porous, connecting different medical traditions.

In the past decades, noninvasive fMRI techniques have opened a "window" into the brain, allowing us to investigate the anatomy and the physiological function involved during acupuncture [1–10]. While a large number of randomized controlled trials are providing growing evidence of the clinical efficacy of acupuncture for the treatment of a variety of medical conditions [11–13], its neurophysiologic action is still elusive. Most current studies have focused on the neural correlates of the acute effects of acupuncture; however, knowledge of the organization of such large-scale cortical networks underlying the action of acupuncture behind the active needle stimulation phase is still lacking. Since acupuncture can provide relief beyond the time at which it is performed [14,15], unraveling the mechanisms involved may further explain the therapeutic effects of acupuncture.

Interest in exploring what happens in the human brain when subjects do not perform cognitively demanding tasks has increased in the past few years. Some research-

* Corresponding author. Tel.: +86 10 82618465; fax: +86 10 62527995.
E-mail address: tian@ieee.org (J. Tian).

1002-0071/$ - see front matter © 2009 National Natural Science Foundation of China and Chinese Academy of Sciences. Published by Elsevier Limited and Science in China Press. All rights reserved.
doi:10.1016/j.pnsc.2008.09.009

ers indicated that even in the task-free state, the brain continuously expends a considerable amount of energy, and external tasks only modestly modulate the effects of such ongoing activity [16–18]. Therefore, as suggested by Raichle and colleagues, in terms of overall brain functions, the ongoing intrinsic activity within various brain systems may be at least as important as the activity evoked by external stimuli [17,18]. More importantly, a recent study reported differences in resting state brain function in people with chronic pain compared with controls, and the authors proposed that this difference in resting state brain activity might reflect the cognitive and affective complications of chronic pain [19]. Therefore, analysis of the resting state connectivity can not only help us to better understand the long-term effects of pain on the brain, but also provide the potential benefits of acupuncture in pain treatments.

The general linear model (GLM) implicitly embodies specific assumptions or requires a priori knowledge about the shapes of the time courses to be investigated [20,21]. For example, in a model-dependent block design for specific visual or motor tasks, the corresponding visual or motor cortical areas are assumed to be activated almost simultaneously. This assumption, however, may be problematic when the precise timing and duration of psychological events cannot be specified a priori, such as testing the acute effects of a new drug or food intake on the brain [22]. According to the theory of traditional Chinese medicine (TCM), acupuncture may induce long-lasting post-administration effects [14]. Therefore, the "off-state" in the block design may still retain some of the effects of acupuncture, which have ideally not returned to a baseline. Therefore, using several stimulation blocks in a short period of time, investigators may not be able to dissociate long-lasting effects from other confounding changes, such as the effect of needle manipulation during the experiment. In the current study, a new experimental paradigm, namely the non-repeated event-related fMRI (NRER-fMRI) design, was implemented.

Previous studies have demonstrated a wide range of brain nuclei activated by acupuncture stimulation. Since these brain regions commonly have high relations with acupuncture, we suppose that these regions may constitute a network activated during acupuncture. In this study, we investigated if such a postulated network existed in the resting brain. If so, how can this network be modulated by external stimulation, such as acupuncture, and what is the physiological relevance of such modulation? To address these questions, we originally adopted a graph theory method to evaluate the dynamic changes in functional connectivity among multiple brain regions from the resting state (RS) to the post-acupuncture resting state (PARS) and post-sham resting state (PSRS). By detecting the differences between these graphs under different states, we can explore the mechanisms by which acupuncture modulates this network.

2. Materials and methods

2.1. Subjects

In order to reduce intersubject variabilities, all participants were recruited from a homogeneous group of 14 college students (seven males, ages of 24.3 ± 1.8). All subjects were right handed and acupuncture naïve. Exclusion criteria were any neurological disorder, any medical disorder that would impact the central nervous system, any contraindications to a high magnetic field, as well as any past or current history of psychiatric disorder, substance abuse or treatment with psychiatric medications. After a complete description of the study was given to all subjects, written informed consent was obtained, as approved by a local institutional review board for human studies.

2.2. Experimental paradigm

According to both the converging clinical reports and the theory of TCM, the effects of acupuncture may induce long-lasting post-administration effects, even for several hours [14]. In the current study, a new experimental paradigm, namely the NRER-fMRI design, was employed to investigate the sustained effects of acupuncture during the post-stimulus period. Both verum manual acupuncture (ACUP) and sham acupuncture (SHAM) experiments consisted of 1.5 min needle manipulations, preceded by a 1 min rest period and followed by 12.5 min of scanning at rest (Fig. 1). To facilitate comparison, we also conducted 12.5 min of rest scanning of all subjects without any stimulus.

The presentation sequence of these three runs was randomized and balanced throughout the subject population, and every subject performed only one run each day. Participants were not informed of the order in which the three runs would be performed, and were told to remain relaxed without engaging in any mental task. To facilitate blinding, we also asked the subjects to keep their eyes closed in order to prevent them from actually observing the procedures. According to the subjects' reports after scanning, all of them affirmed that they had stayed awake during the whole process. At the end of each 15 min scan, the subjects adopted a 10-point scale to self-rate the intensities about the sensations they had felt during the stimulation (0 = no sensation, 1–3 = mild, 4–6 = moderate, 7–8 = strong, 9 = severe and 10 = unbearable sensation). The deqi sensations consist of the following sensations: aching, pressure, soreness, heaviness, fullness, warmth, coolness, numbness, tingling, and dull pain. Since sharp pain was considered to be an inadvertent noxious stimulation [2,3], we excluded subjects from further analysis if they experienced sharp pain (greater than two standard deviations above the mean pain level). In this cohort, no subjects experienced sharp pain.

Acupuncture was performed at acupoint ST 36 on the right leg (Zusanli, located four finger breadths below the

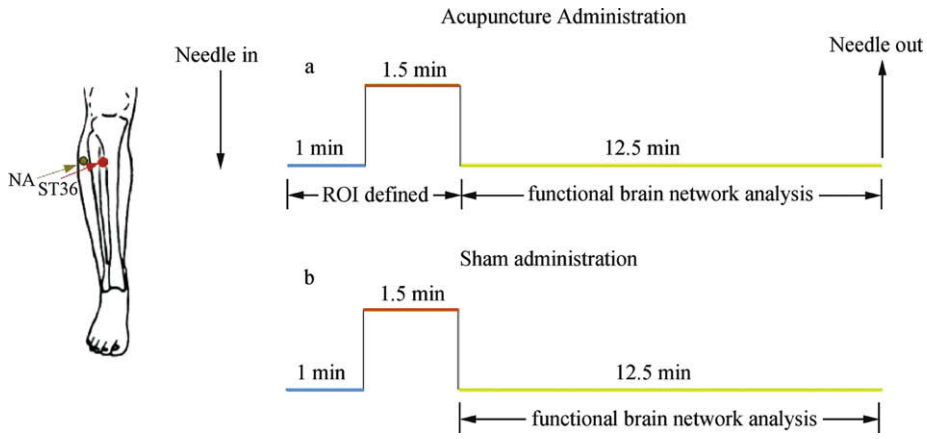

Fig. 1. Experimental paradigm. Panel (a) indicates that the verum acupuncture needle manipulation was performed at acupoint ST 36 on the right leg (Zusanli, arrow pointing to red dot). Panel (b) presents the same design paradigm employed as sham (NA, nonacupoint; 2–3 cm apart from ST 36, arrow pointing to green dot). For statistical analyses, the signal intensity during the 1 min rest phase served as a control baseline for detecting the changes in signal intensity during acupuncture stimulation, thereby functionally defining the regions of interest. In addition, the data from the 12.5 min rest phase were used for further connectivity analysis.

lower margin of the patella and one finger breadth laterally from the anterior crest of the tibia). This is one of the most frequently used acupoints for pain analgesia and disorders of multiple systems. Acupuncture stimulation was delivered using a sterile disposable 38-gauge stainless steel acupuncture needle, 0.2 mm in diameter and 40 mm in length. The needle was inserted vertically to a depth of 2–3 cm, and administration was delivered by a balanced "tonifying and reducing" technique. Stimulation consisted of rotating the needle clockwise and counterclockwise for 1 min at a rate of 60 times per min. The procedure was performed by the same experienced and licensed acupuncturist on all the subjects.

Since the effect of acupuncture is subject to the amount of improvement from a baseline reading, a control group is essential. In other words, the decision as to which control should be used will ultimately depend on the particular question that the research model plans to answer. In the current study, we used sham acupuncture as a control model, and focused on the point specificity (acupoint vs. non-acupoint) of acupuncture. Sham acupuncture was initially devised with needling at nonmeridian points (2–3 cm away from ST 36) with needle depth, stimulation intensity, and a manipulation method identical to those used in verum acupuncture. Similarly, PSRS data were collected for further connectivity analysis.

2.3. Data acquisition and analysis

Images were obtained on a 3-T GE Signa scanner using a standard GE whole head coil (LX platform, gradients 40 mT/m, 150 T/m/s, GE Medical Systems, Milwaukee, Wisconsin). A custom-built head-holder was used to prevent head movement. Thirty-two axial slices (FOV 240 × 240 mm, 64 × 64 matrix, 5 mm thickness), parallel to the AC-PC plane and covering the whole brain were acquired using a $T2^*$-weighted single-shot, gradient-recalled echo planar imaging (EPI) sequence (TR 1500 ms, TE 30 ms, 90° flip angle). The scan covered the entire brain, including both the cerebellum and the brainstem. Prior to the functional run, high-resolution structural information on each subject was acquired using 3D MRI sequences with a voxel size of 1 mm^3 for anatomical localization.

All preprocessing steps were carried out using statistical parametric mapping (SPM5, http://www.fil.ion.ucl.ac.uk/spm/). Because of the instability of the initial signals and to allow for the subjects' adaptation to the situation, the first 10 images were discarded. The remaining images were first corrected for within-scan acquisition time differences between slices and then realigned to the first volume to correct for head motions (none of the subjects had head movements exceeding 1 mm on any axis or head rotation greater than one degree). The image data were further processed with spatial normalization based on the MNI space and re-sampled at 2 × 2 × 2 mm. Global means and linear trends were removed throughout each functional volume to eliminate both global correlation and gross signal drifts using Gramm-Schmitt orthogonalization [23]. Subsequently, functional images were spatially smoothed with a 6-mm FWHW Gaussian kernel.

The low-frequency components of the fMRI time series have been shown to have interregional correlations between functionally related brain areas [24]. A finite-impulse response band-pass filter was applied to the dataset used for functional connectivity analyses to remove the signals in the frequency range out of the 0.01–0.1 Hz range.

2.4. Definition of ROIs

Given that the sustained effects of acupuncture may continue into the post-stimulus period, the mean signal intensity of the resting period preceded by the active stimulation served as the baseline. Then, the difference in the blood

oxygen level-dependent response between stimulus and baseline conditions was estimated at every voxel across the whole brain volume, for each individual subject, using the general linear model in SPM5. The generated *t*-maps at individual levels were then entered into the "random-effect" group analysis framework by the one-sample *t*-test ($df = 13$) summary statistic ($P < 0.001$, uncorrected). The statistical maps indicated the brain activation in response to acute acupuncture stimuli, thereby functionally defining the regions of interest. The peak voxel and its nearest 10 neighbors were defined as a group ROI. These group ROIs were used to define subject-specific ROIs.

Taking into account the anatomical variance across subjects, subject-specific peak voxels and subject-specific ROIs were defined on individual *t*-maps as follows. A given group ROI was first used as a mask. Then, based on the individual *t*-map, the voxel with the largest *t*-value within this mask was taken as the subject-specific peak voxel. The time courses of voxels within the ROI were averaged to generate a single low-frequency reference time series (node time series for further analysis). In clinical practice, ST 36 is the most frequently used acupoint in Chinese acupuncture, especially for analgesia or other treatment of pain. ROIs were selected based on the acupuncture-stimulation results, and these covered almost all the related nuclei reported in the previous studies on acupuncture ST 36 [3,7]. In this manner, we obtained a total of 21 ROI time series related to acupuncture stimulation for each subject.

2.5. Large-scale connectivity identified by a graph theory model

In this study, we used a network model based on graph theory to describe the functional connectivity in the resting brain [25]. The nodes of the network denote the brain regions, and the links describe the connections or information flow among them. In order to measure the connectivity degree η_{ij} between nodes i and j, we used one of the simplest ways which is exponentially related to the distance between them, namely, $\eta_{ij} = \exp(-\xi d_i)$, where ξ is a real positive constant, measuring how the strength of the relationship decreases with the distance between the two nodes (ξ is a subjective selection as discussed by Lopez and Sanjuan [26] and it is here fixed to $\xi = 2$), and d_{ij} is the distance between the two nodes, calculated as a hyperbolic correlation measure. This calculation is as follows: $d_{ij} = (1-c_{ij})/(1 + c_{ij})$, where c_{ij} represents the Pearson correlation coefficient between the two nodes (that is, cross-correlating two of the averaged time series described above). In this way, we can define the total connectivity degree Γ_i of a node i in a graph as the sum of all the connectivity degrees between node i and all the other nodes, specifically, $\Gamma_i = \sum_{i=1}^{n} \eta_{ij}$. This equation describes the amount of information node i receives from the particular network. In this context, a larger Γ means that this region is more functionally connected to other regions in this network. In other words, this node is more important in this network. Thus, it is possible to find the changes in the total functional connectivity network by detecting Γ of some specific regions under different brain activity states.

For each subject, three preprocessed datasets, including PARS, PSRS and RS, were implemented with this graph theory method. We normalized Γ_i of a node i by $\bar{\Gamma}_i = \Gamma_i / \sum_j^n \Gamma_i$ for the comparison among different datasets. The normality distribution of $\bar{\Gamma}$ values under each state was tested using the kurtosis test. Through tracking the changes in functional connectivity degree for each ROI, we can determine what modulation patterns are involved in the effects of acupuncture. Differences in $\bar{\Gamma}$ within the ROIs in the three resting states were tested by ANOVA. Paired *t*-tests were also implemented to identify the differences between PARS and RS, and between PSRS and RS.

3. Results

3.1. Psychophysical response

The prevalence of these sensations (Deqi) was expressed as the percentage of individuals in the group who reported a given sensation (Fig. 2a). The intensity is expressed as the average score ± SE (Fig. 2b). Fullness led the list in the frequency of occurrence during acupuncture, followed by soreness, numbness, aching and dull pain. Although sensations such as soreness, numbness and fullness occurred at higher rates among subjects undergoing acupuncture stim-

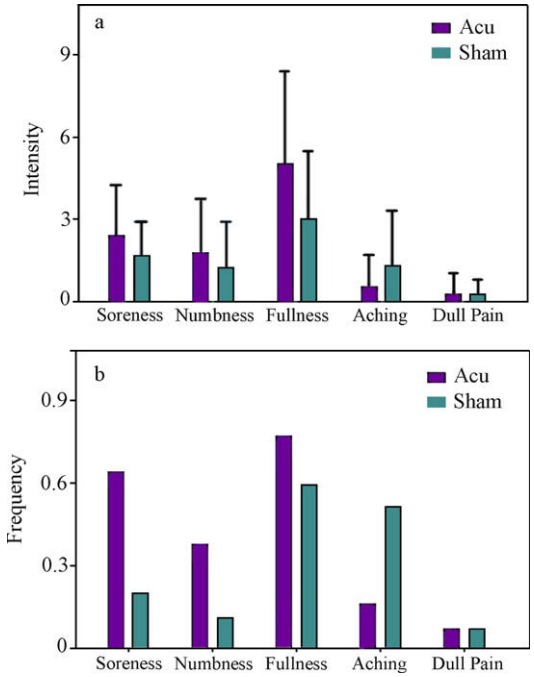

Fig. 2. Psychophysical ratings averaged across 14 subjects. (a) The averaged index of pain experienced by all the participants. Significant differences in soreness, fullness, numbness and aching were observed following verum acupuncture stimulation compared with sham stimulation. Error bars show 95% confidence intervals. (b) The frequency of sensations occurring among all subjects.

ulation than among those undergoing sham intervention no significant differences in the overall frequency of experience were found between acupuncture and sham stimulation control conditions (Fisher's exact test, $P > 0.05$). The level of sensation was kept low (mild to moderate) throughout these two conditions. Average ratings of the reported five elements of Deqi sensations fell between 0 and 4.0 on the 10.0-point scale for both ACUP and SHAM. The highest scores in individual cases were mainly distributed in the range 3 to 8.

3.2. Brain region response evoked by the acupuncture stimulation

The brain regions showing signal changes during acupuncture stimulation are presented in Fig. 3. For bilaterally activated regions, we only selected the hemisphere anatomical area with the more significant t value as the representative ROI. Finally, 21 brain regions were selected as the nodes of the graph further to the connectivity analysis shown in Table 1.

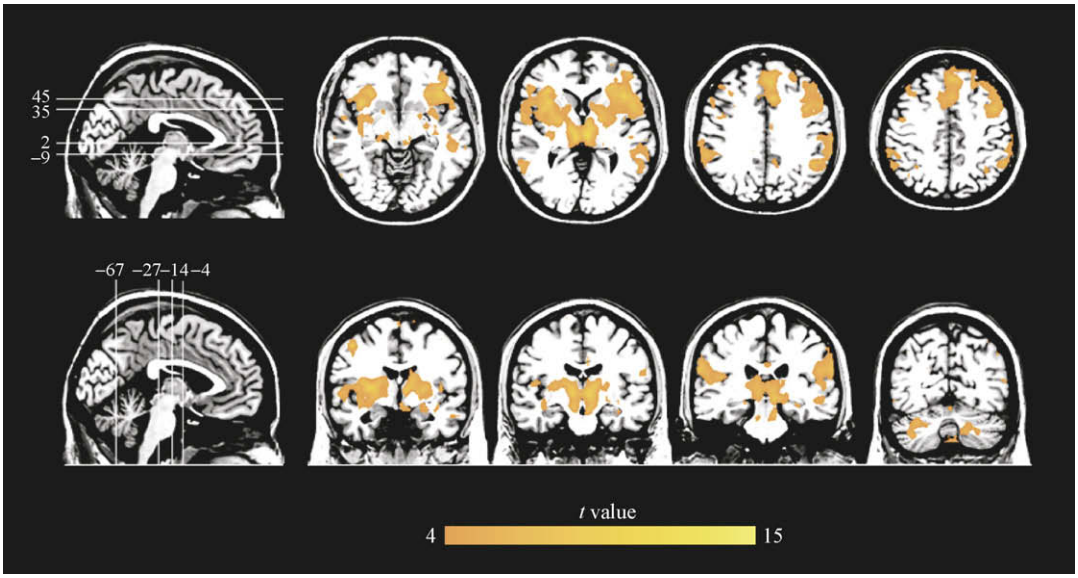

Fig. 3. Group activation t-map for acupuncture ($P < 0.001$, uncorrected, clusters with size > 5 voxels). Representative color-coded statistical maps showing the distribution of foci with significant increases (shown in the spectrum from orange to yellow).

Table 1
Coordinates and t scores of the peak voxel within group ROIs following acupuncture.

Regions	Hem	BA	Talairach			t-value
			x	y	z	
Amygdala (AMY)	R		21	−1	−18	4.28
Hippocampus (HIPP)	R		30	−12	−15	3.79
Parahippocampus (PHIP)	L	34	−21	−24	−9	4.71
Anterior cingulate cortex (ACC)	R	32	6	33	20	6.71
Posterior cingulate cortex (PCC)	R	29	6	−46	16	4.49
Insula	R	13	39	20	2	8.49
Hypothalamus (HYPO)	R		3	−6	−4	5.81
Nucleus accumbens (NA)	R		18	27	18	4.67
Thalamus (Tha)	R		6	−23	4	12.53
Caudate	L		15	4	14	4.74
Putamen	L		−27	−6	6	8.98
Periaqueductal gray (PAG)	R		3	−30	−8	4.34
Paracentral lobule (PRCL)	L	2	−45	−5	9	4.96
Supplementary motor area (SMA)	R	6	8	23	48	7.23
Secondary somatosensory cortex (SII)	L	40	−57	−22	18	6.15
Medial frontal cortex (MFG)	R	8	9	37	45	11.36
Superior frontal cortex (SFG)	R	10	36	56	14	10.61
Inferior parietal cortex (IPC)	R	40	59	−34	24	10.15
Precuneus (PRCN)	R	31	9	−48	33	4.38
Declive	R		−12	−80	−21	11.54
Culmen	L		−3	−56	−17	4.22

Abbreviations: BA—Brodmann area; Hem—hemisphere.

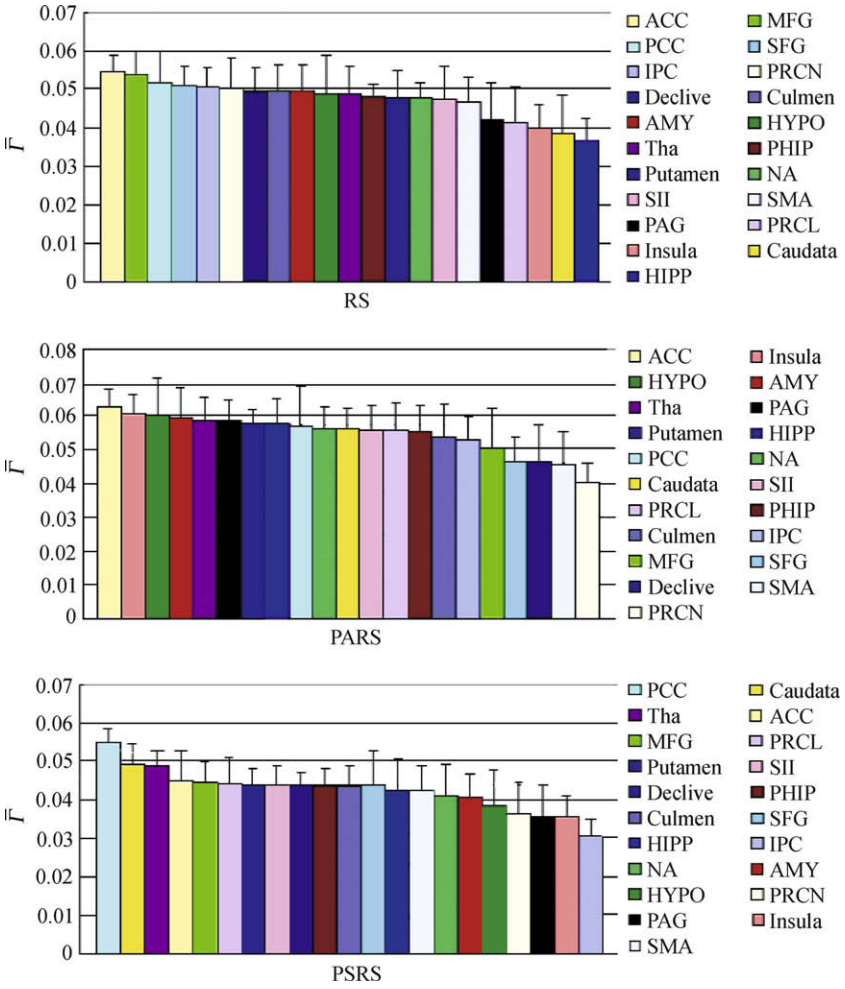

Fig. 4. Ranking of the selected brain regions based on their $\bar{\Gamma}(\pm SD)$ values across all subjects. The brain regions with larger $\bar{\Gamma}$ values are considered to be important nodes in the resting state of the functional connectivity network.

3.3. The functional connectivity network detected by the graph theory model

The results of total connectivity degrees for each ROI during the three resting states are presented in Fig. 4. A larger $\bar{\Gamma}$ indicated significant functional connectivity between this brain region and others; thus, such regions were considered important nodes in this network. In the case of the RS, the regions with the eight highest $\bar{\Gamma}$ values were as follows: ACC, MFG, PCC, SFG, IPC, PRCN, declive, and culmen (Fig. 4a). In the PARS, the regions with the eight highest $\bar{\Gamma}$ values were mainly located in the limbic system (Fig. 4b), such as the ACC, insula, HYPO, AMY, Tha, PAG, putamen, and HIPP. In the PSRS, the regions with the eight highest $\bar{\Gamma}$ values were: PCC, caudate, Tha, ACC, MFG, PRCL, putamen, and SII (Fig. 4c).

For these states, $\bar{\Gamma}$ values had an approximate Gaussian distribution (kurtosis test: kurtosis = 3.56; Gaussian distribution, kurtosis = 3). Differences in $\bar{\Gamma}$ among ROIs during RS ($F_{20,\ 478} = 1.52$, $P < 10^{-4}$), PARS ($F_{20,\ 478} = 2.36$, $P < 10^{-7}$), and PSRS ($F_{20,\ 478} = 1.79$, $P < 10^{-5}$) were tested. With strict Bonferroni correction (namely, $0.05/21 \approx 0.0024$ as a threshold), a paired *t*-test showed significant differences in $\bar{\Gamma}$ for ROIs either for PARS vs. RS or for PSRS vs. RS comparisons (Fig. 5). Trends toward increases in the insula, HIPP, putamen, PAG, caudate, HYPO and AMY, and decreases in the declive, PCC and SFG were observed during PARS in contrast to RS. Meanwhile, our findings also presented an increased tendency in the caudate, Tha, HIPP, SFG, and SMA, but a decreased propensity in the IPC, PRCN, and HYPO during PSRS compared with RS.

4. Discussion

In this paper, we demonstrated a set of brain regions activated by acupuncture stimulation which also exhibit high temporal coherences in the absence of a stimulus resting period. More importantly, our findings also indicated changes in the network under different states, from RS to PARS or from RS to PSRS, suggesting that the functional connectivity of this network maintains a dynamic equilibrium and is reorganized by exerting distinct functions on the human brain.

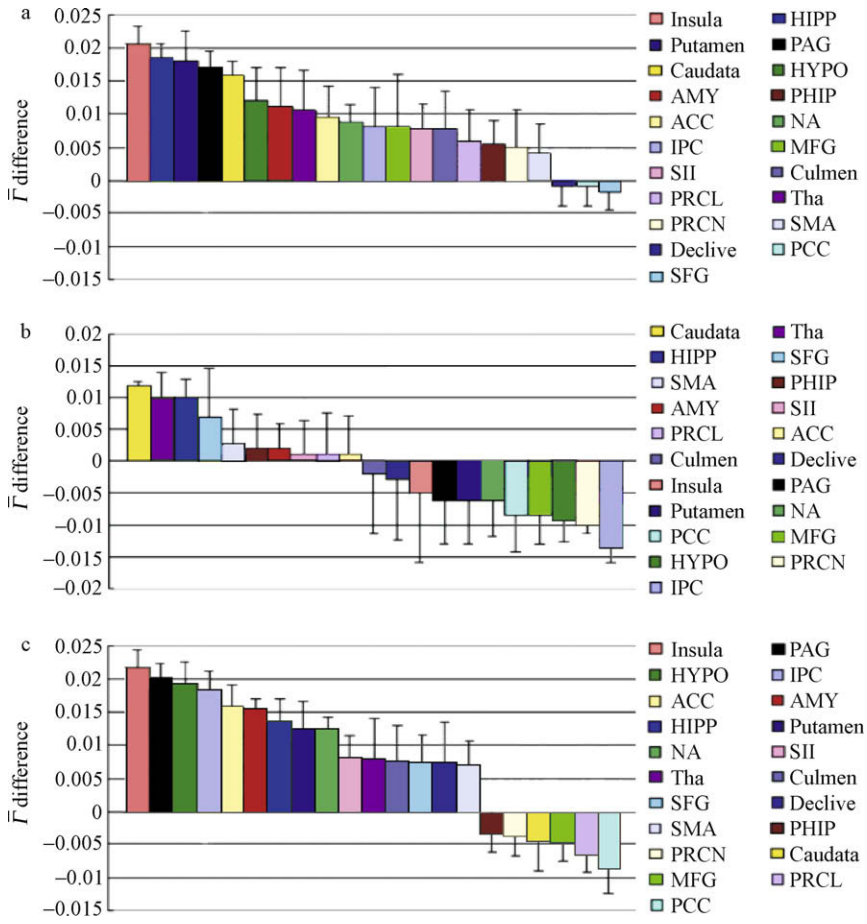

Fig. 5. Differences in $\bar{\Gamma}$ (paired t-test, $P < 10^{-4}$). (a) PARS vs. RS; (b) PSRS vs. RS; (c) PARS vs. PSRS.

Recently, increasing attention has been focused on detecting interregional connectivity in the resting state, which is usually described in terms of functional connectivity. It should be noted that the previously used standard functional connectivity analysis primarily focused on the correlation patterns between a specific region (so-called "seed") and other brain structures, depicting a network related to one certain brain function. Although seed voxel(s) analysis can identify brain regions functionally connected to the initially selected seed, it is unable to completely characterize the joint interactions among multiple brain regions. By the graph mode with n-to-1 connectivity instead of conventional pairwise connectivity analysis, not only can we use connectivity degrees to quantify the importance of nuclei implicated in the network, but also we can investigate the network modulation patterns by detecting the changes in the nuclei connectivity graph under different states. Under the construct of this network model, some brain regions with a larger degree of connectivity indicated stronger interactions with other brain regions and were considered to be important nodes in this network.

In the case of the RS, the significant nodes in the network, including the ACC, MFG, PCC, IPC, and precuneus, showing task-independent, stimulus-induced deactivations, underlie a "default mode" of brain activity [27–29]. The precise function of the default mode network is debated, but evidence suggests that it may support autobiographical memory and decreased externally focused attention [30]. In other words, during a novel and specific task, processing resources are moved from the areas normally engaged in the "default mode" to the areas relevant for the presented task. Acupuncture, as a peripheral input to transducing signals into the brain, may induce the reorganization of the functional connectivity across different subsystems. The previous neuroimaging studies of the acute effects of acupuncture have demonstrated its significant modulatory effect on the limbic system, paralimbic and subcortical gray structures [2,3,7,8]. This conclusion was also corroborated by our findings: this acupuncture-related network was mainly distributed in the limbic and subcortical systems, including ACC, insula, HYPO, AMY, HIPP, Tha, and PAG. These areas, which largely overlap with the "pain matrix", such as pain-sensory (Tha), pain-affective (ACC, AMY, HIPP), and pain-modulation (insula, HYPO, PAG) regions, are the main modulating structures associated with the release of neurotransmitters (such as endogenous opioids) in acupuncture-induced analgesia.

If the network during rest can be modulated by acupuncture, we expect that there exist significant differences in connectivity degree among specific brain regions

between the resting state and the post-acupuncture resting state. This hypothesis is strongly supported by the results of the paired *t*-test shown in Fig. 2. The $\bar{\Gamma}$ values for insula, HIPP, PAG, HYPO, AMY and ACC showed a trend toward an increase during the PARS compared with RS (Fig. 2a). BOLD signal changes in insula were the most consistently observed findings regardless of acupoint location or acupuncture mode [1,2,5–10]. With abundant connections and functional interface between the limbic system and the neocortex, the insula cortex plays a key role to assign significance to the sensory information it receives [31,32], possibly to effect decisions and subsequent behavior [33,34]. This finding also demonstrated that the limbic system participates in pain perception, particularly the affective-cognitive aspect. Anatomy and neurophysiology researchers have discovered that amygdala nuclei with abundant afferent and efferent nerve fibers can receive and integrate different elements of sensory projection information, and have extensively mutual contact with other cortical and subcortical structures, which play an important role in acupuncture [34,35]. Hippocampal activity can be strongly modulated by means of both pain and acupuncture stimulation [36,37]. Furthermore, the ACC, which has extensive connections to the amygdala and periaqueductal gray matter, is a key modulator of the internal emotional response to pain [38]. According to our findings, the increased connectivity between certain nuclei shows that these nuclei became more important in this network following acupuncture. The finding of this increased connectivity between these structures, together with the HYPO, is consistent with the results of animal experiments supporting the notion that acupuncture afferent pathways engage the structures of the descending antinociceptive system [37,39,40].

It should be noted that ACUP and SHAM may exert a different modulation pattern on the resting brain network (Fig. 5a and b). In the case of PARS vs. RS, the significance of some brain regions indicated a prominently ascending tendency, mainly in the insula, HIPP, PAG, and AMY (Fig. 5a). By contrast, such notable ascending propensity in the PSRS vs. RS comparison was primarily located in the caudate, Tha, HIPP and MFG (Fig. 5b). Moreover, this varied pattern became more salient in the PARS vs. PSRS comparison (Fig. 5c). In the case of the PARS vs. PSRS comparison, the significance of most brain regions indicated a significantly ascending tendency in the insula, PAG, HYPO, IPC, ACC, and AMY, but an opposite direction in PCC, PRCL, MFG, caudate, PRCN and PHIP. Although some evidence from acupuncture studies have indicated significant overlaps of the "pain-matrix" involved in the acupuncture and sham stimulations, our result clearly demonstrated that acupuncture and sham may exert different modulation patterns on this network. Although it is difficult for us to interpret the concrete modulation mechanism in the current study, this study may provide a step toward the exploration of the curative effects of acupuncture in clinical settings.

It is important to emphasize that the changes in the interactions among brain regions reflect the changes in the network functions. Thus, various networks can participate in and implement different human brain activities. In this study, we implemented an ANOVA to evaluate the connectivity strength of the network under different states: $F_{20,\ 478} = 1.52$ (RS), $F_{20,\ 478} = 2.36$ (PARS), $P < 10^{-4}$. These findings provide compelling evidence to support the existence of acupuncture modulation on the acupuncture-related network. Moreover, these nuclei altered from having looser connectivity links to having a more compact connectivity network, implying the accomplishment of acupuncture function. As shown above, the brain's functional connectivity is highly flexible and can be modulated by external or internal environmental changes. It is the altered process that implements different brain functions under different brain states. The results of our study imply that the therapeutic effects of acupuncture may depend on the modulation of certain brain areas related to special disorder treatment. Thus, our study can be considered as fully assessing joint interaction among multiple brain regions in different states of brain activity, which may be helpful to understanding the basic neurophysiological mechanisms underlying the effects of acupuncture. It should also be noted that this approach relies particularly on the existence of a neural theoretical framework and is often limited by the nodes (regions) of interest. Further investigation and clarification of the mechanisms underlying the effects of acupuncture are required.

Acknowledgements

This work is supported by the Project for the National Key Basic Research and Development Program (973; grant no. 2006CB705700), Changjiang Scholars and Innovative Research Team in University (PCSIRT; grant no. IRT0645), Chair Professors of Cheung Kong Scholars Program, CAS Hundred Talents Program, CAS Scientific Research Equipment Develop Program (YZ0642, YZ200766), Joint Research Fund for Overseas Chinese Young Scholars (grant no. 30528027), National Natural Science Foundation of China (grant no. 30873462, 90209008, 30870685, 30672690, 30600151, 60532050, 60621001), and the Beijing Natural Science Fund (grant no. 4071003).

References

[1] Fang JL, Krings T, Weidemann J, et al. Functional MRI in healthy subjects during acupuncture: different effects of needle rotation in real and false acupoints. Neuroradiology 2004;46:359–62.

[2] Hui KKS, Liu J, Makris N, et al. Acupuncture modulates the limbic system and subcortical gray structures of the human brain: evidence from fMRI studies in normal subjects. Hum Brain Mapp 2000;9:13–25.

[3] Hui KKS, Liu J, Marina O, et al. The integrated response of the human cerebro-cerebellar and limbic systems to acupuncture stimulation at ST36 as evidenced by fMRI. Neuroimage 2005;27:479–96.

[4] Liu WC, Feldman SC, Cook DB, et al. fMRI study of acupuncture-induced periaqueductal gray activity in humans. Neuroreport 2004;15:1937–40.
[5] Napadow V, Makris N, Liu J, et al. Effects of electroacupuncture versus manual acupuncture on the human brain as measured by fMRI. Hum Brain Mapp 2005;24:193–205.
[6] Pariente J, White P, Frackowiak RSJ, et al. Expectancy and belief modulate the neuronal substrates of pain treated by acupuncture. Neuroimage 2005;25:1161–7.
[7] Wu MT, Hsieh JC, Xiong J, et al. Central nervous pathway for acupuncture stimulation: localization of processing with functional MR imaging of the brain—preliminary experience. Radiology 1999;212:133–41.
[8] Wu MT, Sheen JM, Chuang KH, et al. Neuronal specificity of acupuncture response: a fMRI study with electroacupuncture. Neuroimage 2002;16:1028–37.
[9] Yoo SS, Teh EK, Blinder RA, et al. Modulation of cerebellar activities by acupuncture stimulation: evidence from fMRI study. Neuroimage 2004;22:932–40.
[10] Zhang WT, Jin Z, Cui GH, et al. Relations between brain network activation and analgesic effect induced by low vs. high frequency electrical acupoint stimulation in different subjects: a functional magnetic resonance imaging study. Brain Res 2003;982:168–78.
[11] National Institutes of Health. Question 1. NIH consensus development statement on complementary medicine; 1997. Available from: odp.od.nih.gov/consensus/statements/cdc/107/107stmt.html.
[12] Ernst E, White A. Acupuncture—a scientific appraisal. Oxford: Butterworth; 1999.
[13] Stux G, Hammerschlag R. Clinicial acupuncture. Heidelberg and Berlin: Springer-Verlag; 2001.
[14] Beijing College of Traditional Chinese Medicine. Essentials of Chinese acupuncture. Beijing: Foreign Languages Press; 1980.
[15] Price DD, Rafii A, Watkins LR, et al. A psychophysical analysis of acupuncture analgesia. Pain 1984;19:27–42.
[16] MacLean JN, Watson BO, Aaron GB, et al. Internal dynamics determine the cortical response to thalamic stimulation. Neuron 2005;48:811–23.
[17] Raichle ME, Gusnard DA. Intrinsic brain activity sets the stage for expression of motivated behavior. J Comp Neurol 2005;493:167–76.
[18] Raichle ME, Mintun MA. Brain work and brain imaging. Annu Rev Neurosci 2006;29:449–76.
[19] Baliki MN, Geha PY, Apkarian AV, et al. Beyond feeling: chronic pain hurts the brain, disrupting the default-mode network dynamics. J Neurosci 2008;28:1398–403.
[20] Duann JR, Jung TP, Kuo WJ, et al. Single-trial variability in event-related BOLD signals. Neuroimage 2002;15:823–35.
[21] McKeown MJ, Makeig S, Brown GG, et al. Analysis of fMRI data by blind separation into independent spatial components. Hum Brain Mapp 1998;6:160–88.
[22] Liu YJ, Gao JH, Liotti M, et al. Temporal dissociation of parallel processing in the human subcortical outputs. Nature 1999;400:364–7.
[23] Lowe MJ. Functional connectivity with continuous state fMRI assessed with structural equations. Neuroimage 1999;9:S197.
[24] Cordes D, Haughton VM, Arfanakis K, et al. Frequencies contributing to functional connectivity in the cerebral cortex in "resting-state" data. Am J Neuroradiol 2001;22:1326–33.
[25] Jiang TZ, He Y, Zang YF, et al. Modulation of functional connectivity during the resting state and the motor task. Hum Brain Mapp 2004;22:63–71.
[26] Lopez L, Sanjuan MAF. Relation between structure and size in social networks. Phys Rev E 2002;65:036107.
[27] Michael DG, Ben K, Allan LR, et al. Functional connectivity in the resting brain: a network analysis of the default mode hypothesis. Proc Natl Acad Sci USA 2003;100:253–8.
[28] Gusnard DA, Raichle ME. Searching for a baseline: functional imaging and the resting human brain. Nat Rev Neurosci 2001;2:685–94.
[29] Raichle ME, Snyder AZ. A default mode of brain function: a brief history of an evolving idea. Neuroimage 2007;37:1083–90.
[30] Buckner RL, Vincent JL. Unrest at rest: default activity and spontaneous network correlations. Neuroimage 2007;37:1091–6.
[31] Mesulam MM, Mufson EJ. Insula of the old world monkey. 111. Efferent cortical output and comments on function. J Comp Neurol 1982;21:38–52.
[32] Casey KL. Forebrain mechanisms of nociception and pain: analysis through imaging. Proc Natl Acad Sci USA 1999;96:7668–74.
[33] Damasio AR, Grabowski TJ, Bechara A, et al. Subcortical and cortical brain activity during the feeling of self-generated emotions. Nat Neurosci 2000;3:1049–56.
[34] Zhou Z, Du M, Wu W, et al. Effect of intracerebral microinjection of naloxone on acupuncture- and morphine analgesia in the rabbit. Sci Sin 1981;24:1166–77.
[35] Manning BH, Mayer DJ. The central nucleus of the amygdala contributes to the production of morphine antinociception in the rat tail-flick test. J Neurosci 1995;15:8199–213.
[36] Khanna S, Sinclair JG. Responses of the CA1 region of the rat hippocampus to a noxious stimulus. Exp Neurol 1992;117:28–35.
[37] Takeshige C. The acupuncture point and its connecting central pathway for producing acupuncture analgesia. Brain Res Bull 1993;30:53–67.
[38] Devinsky O, Morrell MJ, Vogt BA. Contributions of anterior cingulate cortex to behavior. Brain 1995;118:279–306.
[39] Jin WQ, Zhou ZF, Han JS. Electroacupuncture and morphine analgesia potentiated by bestatin and thiorphan administered to the nucleus accumbens of the rabbit. Brain Res 1986;380:317–24.
[40] Wang Q, Mao L, Han JS. The arcuate nucleus of hypothalamus mediates low but not high frequency electroacupuncture in rats. Brain Res 1990;513:60–6.